Geoscience Letters

RESEARCH LETTER

Open Access

Earthquake monitoring of the Baribis Fault near Jakarta, Indonesia, using borehole seismometers

Ruben Damanik[1,2], Pepen Supendi[3,4], Sri Widiyantoro[5,6*], Nicholas Rawlinson[4], A. Ardianto[1], Endra Gunawan[5], Yayan M. Husni[1], Z. Zulfakriza[5], David P. Sahara[5] and Hasbi Ash Shiddiqi[7]

Abstract

The geological setting of Jakarta and its immediate surroundings are poorly understood, yet it is one of the few places in Indonesia that is impacted by earthquakes from both the Java subduction zone and active faults on land. In this study, a borehole seismic experiment with low noise characteristics was deployed to record seismic activity on the ~ E-W oriented Baribis Fault, which is ~ 130 km long, passes to the south of Jakarta, and is only ~ 20 km away at its nearest point. A primary objective of this study is to determine whether this fault is seismically active, and therefore, whether it might pose a threat to nearby population centers, including Jakarta in particular. A total of seven broadband instruments that spanned Jakarta and the surrounding region were installed between the end of July 2019 and August 2020, during which time we were able to detect and locate 91 earthquakes. Two earthquakes were located close to the Baribis Fault line, one of which was felt in Bekasi (southeast of Jakarta) where it registered II-III on the Modified Mercalli Intensity (MMI) scale. The focal mechanism solutions of these events indicate the presence of a thrust fault, which is in good agreement with previous studies, and suggest that the Baribis Fault is active.

Keywords: Indonesia, Seismicity, Active fault, Earthquake

Introduction

Jakarta, the capital city of Indonesia, located in the western Java, is underpinned by a geologically complex terrane that arises from the convergence of the Australian Plate and the Eurasian Plate along the Java Trench. In addition to earthquakes generated along this subduction zone, Jakarta and its surroundings are also affected by earthquakes that rupture on active crustal faults in western Java, such as the Cimandiri Fault (Katili and Soetadi 1971; Setyadji et al. 1997), Lembang Fault (Daryono et al. 2018), Cipamingkis Fault (Gunawan and Widiyantoro 2019), and Garut Faults (Supendi et al. 2018). These active faults are located close to areas with high population densities, such as Jakarta and Bogor. In the case of the Baribis Fault, whose status (seismically active or inactive) is unknown, the result of a previous study using ambient noise tomography (ANT) reveals it as a velocity contrast that passes to the south of Jakarta (Rosalia et al. 2019), which confirms the finding of Simandjuntak and Barber (1996) based on geological mapping (see Fig. 1). Furthermore, based on geodetic constraints from Global Positioning System data, Koulali et al. (2017) produced a kinematic model of convergence of the Australian Plate and the eastern Sunda Arc that involves slip partitioning between the Java Trench and a structure extending nearly E-W across Java. Although most of the convergence is being accommodated by the Java megathrust, the model requires a small component to be accommodated along the Baribis Fault.

The Jakarta Basin, which hosts Indonesia's capital city, has an average elevation of ~ 7 m and a variable

*Correspondence: ilikwidi@gmail.com
[5] Global Geophysics Research Group, Faculty of Mining and Petroleum Engineering, Institut Teknologi Bandung, Bandung 40132, Indonesia
Full list of author information is available at the end of the article

Springer Open

© The Author(s) 2021. **Open Access** This article is licensed under a Creative Commons Attribution 4.0 International License, which permits use, sharing, adaptation, distribution and reproduction in any medium or format, as long as you give appropriate credit to the original author(s) and the source, provide a link to the Creative Commons licence, and indicate if changes were made. The images or other third party material in this article are included in the article's Creative Commons licence, unless indicated otherwise in a credit line to the material. If material is not included in the article's Creative Commons licence and your intended use is not permitted by statutory regulation or exceeds the permitted use, you will need to obtain permission directly from the copyright holder. To view a copy of this licence, visit http://creativecommons.org/licenses/by/4.0/.

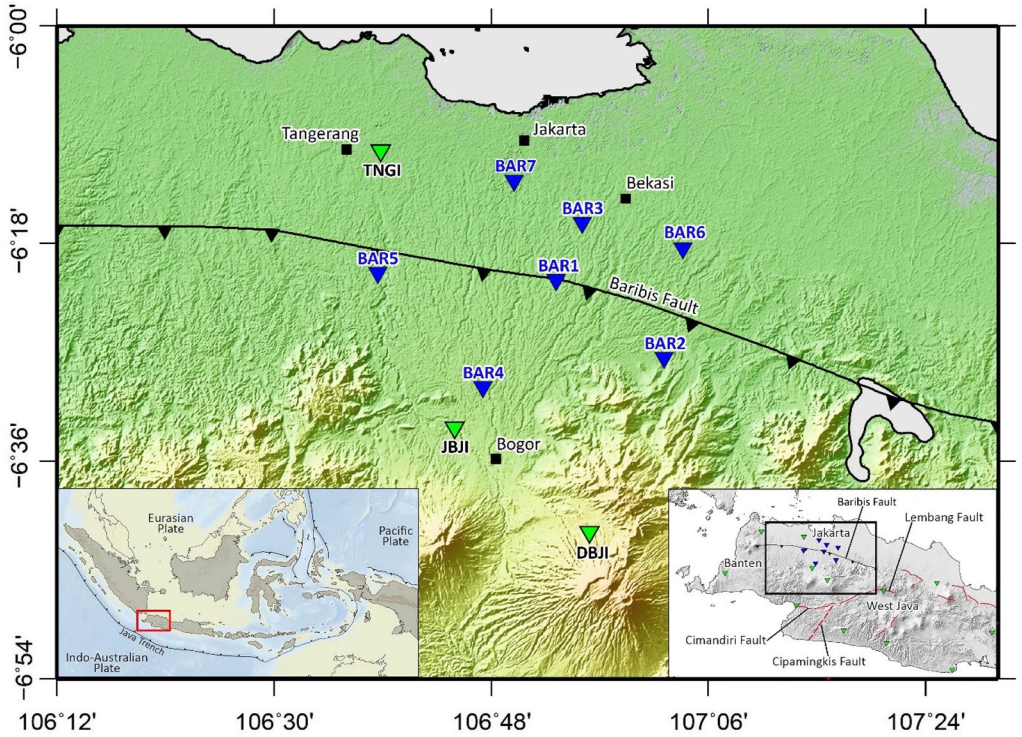

Fig. 1 Map of the study area. Blue and green inverted triangles are the borehole and BMKG seismic stations, respectively, used in this study; black line represents the Baribis Fault extracted from Simandjuntak and Barber (1996); left inset shows the location of the western part of West Java (red rectangle) with respect to the Indonesian region; right inset shows the location of the study area (black rectangle) with respect to the western part of Java. Red lines correspond to the other major crustal faults, including Cimandiri and Lembang Faults which were extracted from Irsyam et al. (2017, 2020) and the Cipamingkis Fault (Gunawan and Widiyantoro 2019)

thickness that ambient noise studies suggest may exceed 1 km in some places (Saygin et al. 2016). Saygin et al. (2017) described an autocorrelation study in Jakarta that revealed the underlying P-wave velocity structure; this was used to infer variations in basement depth beneath the thick sedimentary basin that hosts Indonesia's capital city. Cipta et al. (2018) applied trans-dimensional Bayesian inversion of H/V spectral ratios of fundamental mode Rayleigh waves extracted from the ambient seismic noise wavefield to reveal low seismic velocities beneath the northern to central part of Jakarta, which will potentially contribute to seismic amplification and basin resonance. Ridwan et al. (2016, 2019) defined an engineering bedrock morphology with a depth range of 350–725 m beneath Jakarta, and suggested that the region could be severely affected by nearby earthquakes due to ground motion amplification. Typically, earthquakes felt in the Jakarta area occur on the subducting slab that is part of the northerly migrating Australian Plate. Historically, there are two significant earthquakes that resulted in fatalities and the collapse of buildings in Jakarta; these occurred on January 5, 1699 and January 22, 1780 (Musson 2012; Wichmann 1918). Nguyen et al. (2015) modeled the 1699 event and suggested that a ~ Mw 8.0 earthquake occurred in the subducting slab at a depth of around 160 km. During the 1780 event, 27 structures collapsed in Jakarta (Musson 2012; Wichmann 1918). In a recent seismic study using the regional network of the Meteorology, Climatology, and Geophysics Agency (BMKG) in West Java, Supendi et al. (2018) did not detect much seismicity around Jakarta, likely due to the lack of stations and the presence of high levels of anthropogenic noise. The use of borehole instruments will improve coverage and reduce the detection of such noise, which would permit smaller events to be recorded.

In this study, earthquake monitoring was carried out by deploying seven borehole seismometers (Fig. 1; Table 1) around the Baribis Fault near Jakarta. Despite prior work in this area (e.g., Simandjuntak and Barber 1996 and Rosalia et al. 2019), it is still unclear whether the fault is currently active and may pose a risk to Jakarta.

Data and method

We completed a temporary installation of seven borehole seismometers in July–August 2019, as part of the collaboration between Institut Teknologi Bandung (ITB)

Table 1 The location of seven borehole stations used in this study

Station name	Latitude (deg.)	Longitude (deg.)	Depth (m)
BAR1	−6.3506	106.8891	10
BAR2	−6.4579	107.0383	4
BAR3	−6.2720	106.9257	7
BAR4	−6.4977	106.7880	9
BAR5	−6.3403	106.6429	11
BAR6	−6.3067	107.0640	8
BAR7	−6.2133	106.8317	10

and PT. Resuransi Maipark Indonesia. The two first seismometers were deployed at the end of July 2019. Five more seismometers were then deployed in early August 2019. The station design consists of three-component (3C) C100 wideband seismometers deployed at a depth of between 4 and 11 m below ground level using a PVC pipe (Fig. 2a), and a Sri32L Geobit digitizer placed on the surface in a compact shelter 1 m^3 in size (Fig. 2b and c). The seismometers have a flat response between 10 s and 98 Hz, a sensitivity of 1500 V/m/sec on all components, and the signal is digitized at 32 bit resolution. In this study, a sample rate of 100 sps is used. The drilling of the borehole was assisted by a digger machine, and the mini shelter was made of iron to protect the instruments from theft or damage (Fig. 2c). The borehole seismic stations were powered by 12 Volt 75 Ah lead-acid car batteries, which were replaced approximately every 1.5 months. Examples of 3C seismograms recorded by the borehole stations are shown in Additional file 1: Fig. S1.

To determine the quality of the seismogram data, the average of the recorded noise level was evaluated by computing a probability density function (PDF) and plotting the probabilistic power spectral density (PPSD) (Fig. 3 for borehole stations and Additional file 1: Fig. S2 for BMKG stations; the seismometer frequency responses are shown in Additional file 1: Fig. S3). To do this, we removed the

Fig. 2 Photographs of instrumentation and example field sites. **a** C100 wideband seismometer, **b** Sri32L Geobit digitizer, and **c** borehole instrumentation at BAR6 in Bekasi

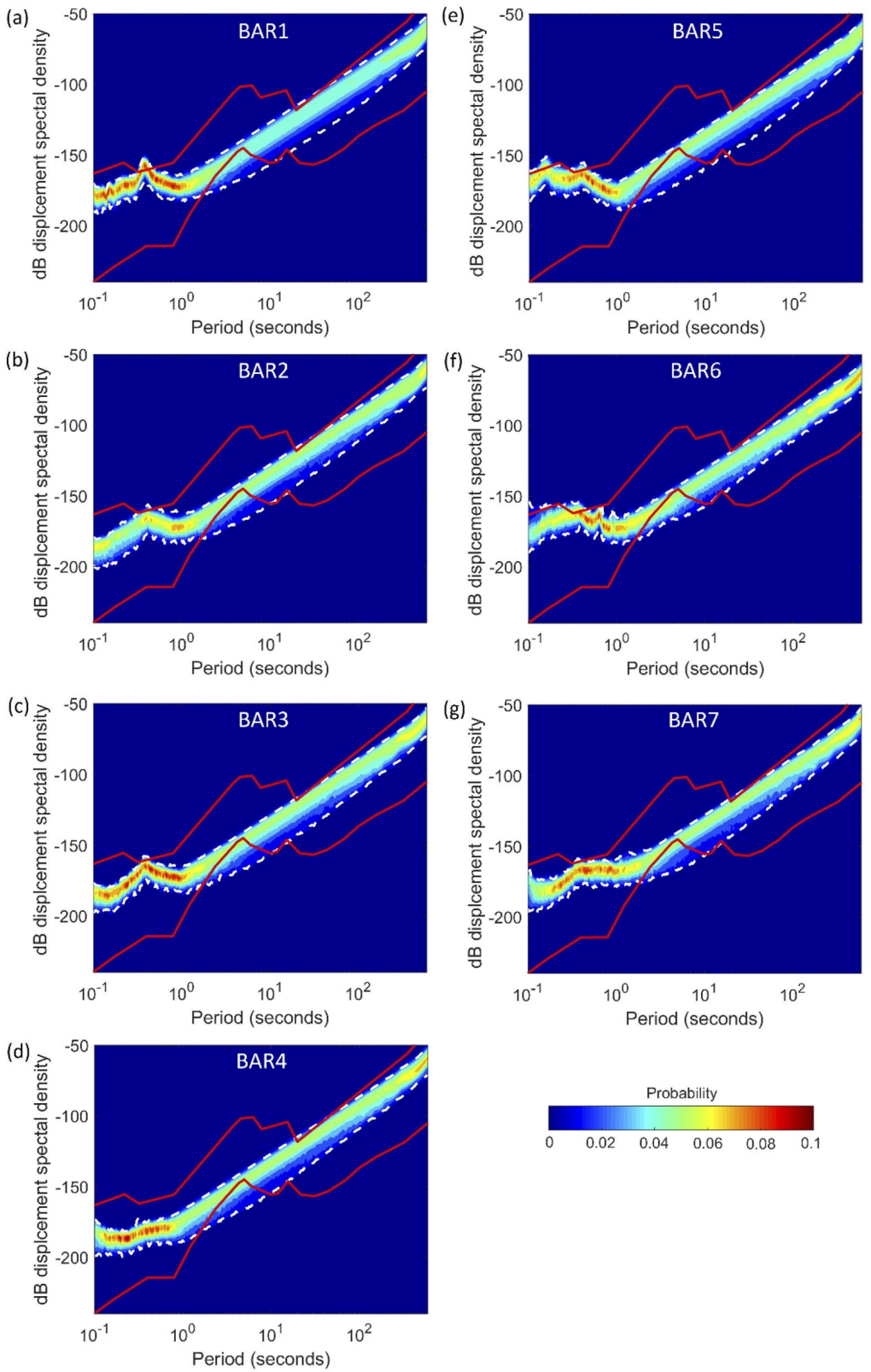

Fig. 3 PPSD for stations **a** BAR1, **b** BAR2, **c** BAR3, **d** BAR4, **e** BAR5, **f** BAR6, and **g** BAR7. Each plot was constructed using 9648 power spectral densities (PSDs) from August to November 2019. White dashed lines indicate the boundaries of 90 percent of the data distribution in each period. Red lines depict high- and low-noise models (Peterson 1993)

mean, detrended, and then deconvolved the instrument response of the seismogram data without prior bandpass filtering. The signal was then windowed using the Hanning tapered window function with a window length of 10 min, making sure that each of these windows did not overlap one another. The PPSD was calculated using a standard FFT algorithm, and the results were interpolated logarithmically. The PPSD results from all windows at each station were then stacked. The PDF was calculated using an adaptive kernel density estimation algorithm based on a linear diffusion process (Botev and Grotowski 2010). The PDF creation process was done iteratively to obtain the optimal bandwidth by considering the most common linear diffusion with the same stationary density as the estimated pilot density. The program for calculating PDFs with adaptive kernel density estimates was created by Botev (2016) and calculations were performed using the vertical component seismograms (BHZ) only.

Data processing was then carried out using two stages: (i) event identification using the FilterPicker Algorithm (Lomax et al. 2012) and (ii) manual picking of P- and S-wave arrival times of 3-component waveforms using Seisgram2K (Lomax and Michelini 2009). The earthquake hypocenters were then determined using the Hypoellipse software (Lahr 1979). Hypoellipse uncertainties are derived from the joint hypocentral confidence region by projecting the joint hypocentral error ellipsoid onto the corresponding regions and by scaling the major axis with the corresponding ratios of the χ^2 value for the different degrees of freedom (Lahr 1989). Fitting of the displacement spectrum amplitude was done using a Brune-type model (Havskov and Ottemöller 2010) to calculate the moment magnitude (Mw), and the ISOLA package (Sokos and Zahradnik 2008) was used to perform moment tensor inversion from the borehole and BMKG seismic stations (see inverted blue and green triangles in Fig. 1). For determining the focal mechanisms, the observed waveforms were pre-processed using a bandpass filter of 0.04 Hz to 0.09 Hz. The data processing stage of focal mechanism analysis is as follows: (i) conversion of data from SAC to ASCII format; (ii) input of the earthquake hypocenter location (longitude, latitude, and depth) and origin time; (iii) station selection; (iv) removal of instrument response, trial seismic source depth, and (v) Green's function calculation using the discrete wavenumber method (Bouchon 1981) to create a synthetic signal based on the velocity model. The match between the observed and best-fitting synthetic data is characterized by the overall variance reduction. The time window chosen for each waveform starts from the event origin time, and ends when the earthquake signal is no longer visible above the background noise. For hypocenter relocation and focal mechanism determination, we used the 1-D seismic velocity model from Koulakov et al. (2007) combined with AK135 (Kennett et al. 1995). As of August 2020, the array had recorded 43 local earthquakes inland and 48 regional earthquakes in the southern part of West Java (Additional file 1: Figs. S4 and S5). We successfully calculated the moment magnitude of a subset of 82 events as listed in Table S1, after requiring a signal-to-noise ratio > 2.0 to ensure good quality results.

Results and discussion

The background noise levels from the seven borehole stations are shown in Fig. 3. The PPSD shows that all stations provide similar results for periods greater than 50 s. Differences between stations were observed at shorter periods; this likely represents different levels of anthropogenic noise between stations. Station BAR4 had the lowest level of anthropogenic noise, whereas the highest was at Station BAR6. Generally, the range of differences in the noise level of each borehole station is relatively small compared with installations on the surface (see, e.g., Miller et al. 2016), which indicates the effectiveness of this approach in reducing noise contamination. Figure 4 shows an example comparison of waveforms from borehole and BMKG surface stations. The seismic waveforms recorded by both kinds of seismometer are quite consistent, although the borehole seismometers appear to be less noisy.

We detected and located 91 earthquakes from one year of data, which together yielded a total of 489 and 458 P- and S-wave arrival times, respectively. To check the reliability of the hypocenter solutions, a Wadati diagram of arrival times was plotted (Fig. 5). In general, a Vp/Vs ratio of 1.75 was obtained. This value is close to the global average Vp/Vs for crust which is 1.73 (Stein and Wysession 2003), indicating that our picking of P- and S-wave arrival times was robust. We plotted the magnitude–frequency relation (Fig. 6) for earthquakes recorded by the borehole stations in the neighborhood of the array. Comparison with equivalent results from the existing regional stations from BMKG shows that the magnitude completeness (Mc) of our borehole stations is lower than the Mc of the BMKG stations, indicating that the borehole array can record smaller events.

Generally, the earthquake hypocenter locations determined from borehole and BMKG stations are divided into local and regional earthquakes with magnitudes ranging from Mw 2.4 to Mw 5.5. Local earthquakes are located inland, while regional earthquakes are located in the southern part of Banten and West Java (Fig. 7a). Uncertainties and travel-time residuals associated with hypocenter location of all events recorded by the borehole and BMKG stations are shown in Additional file 1:

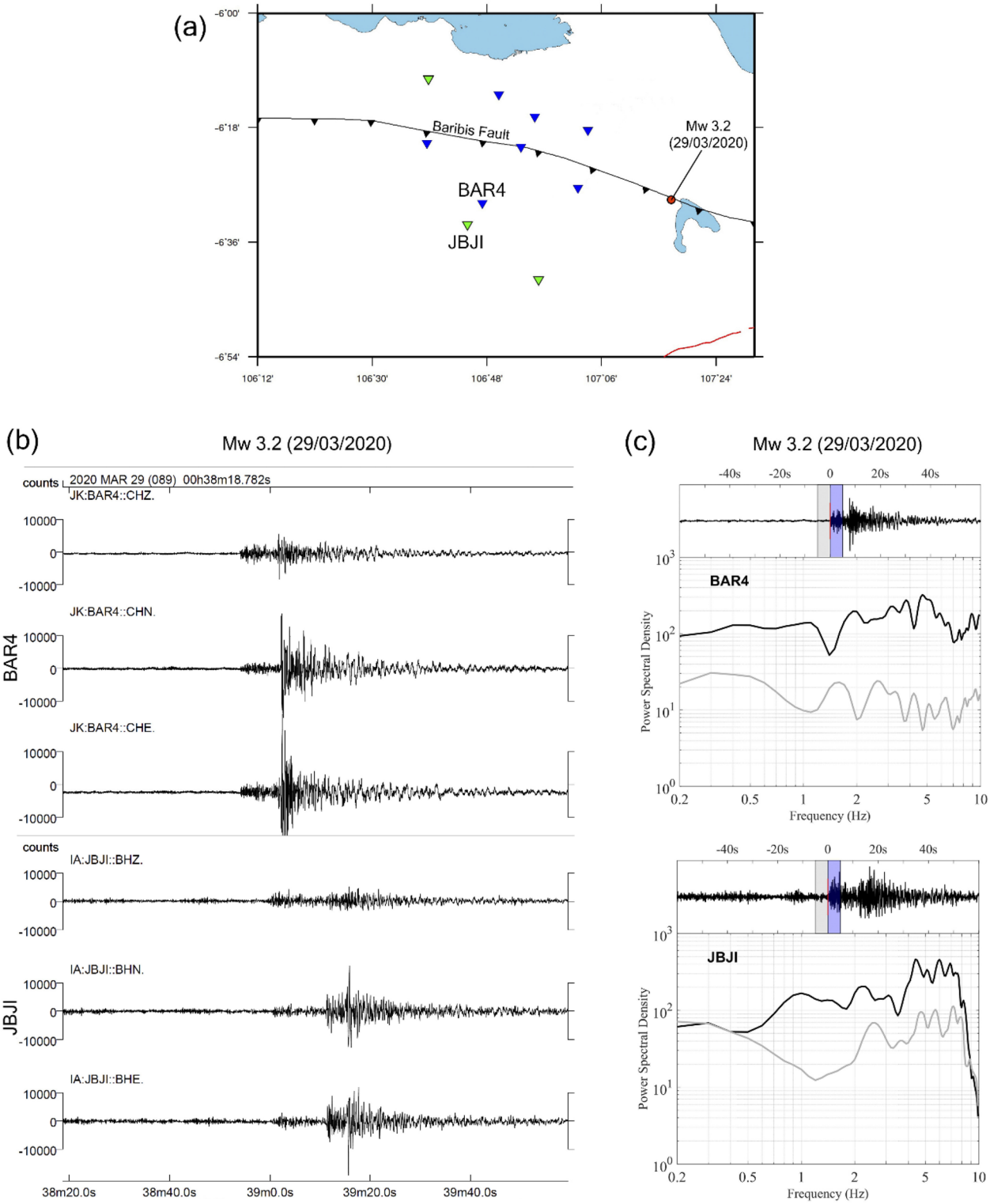

Fig. 4 **a** Map of event and stations used in the comparison of waveform and spectrum of an earthquake (Mw 3.2 on March 29, 2020) at adjacent BMKG (JBJI) and borehole (BAR4) stations. **b** The earthquake waveforms. **c** The corresponding spectrum. We show normalized time series of vertical component seismogram (top panel) and the evaluated signal and noise spectra (bottom panel). The window length used in the calculation of the noise and signal spectra are 5 s before and 5 s after the P-wave arrival time, respectively. In the top panel the signal window is represented as a blue shaded window, while noise is enclosed by a gray shaded window. In the spectrum panel, the gray curve represents the noise spectrum and the black curve is the signal spectrum

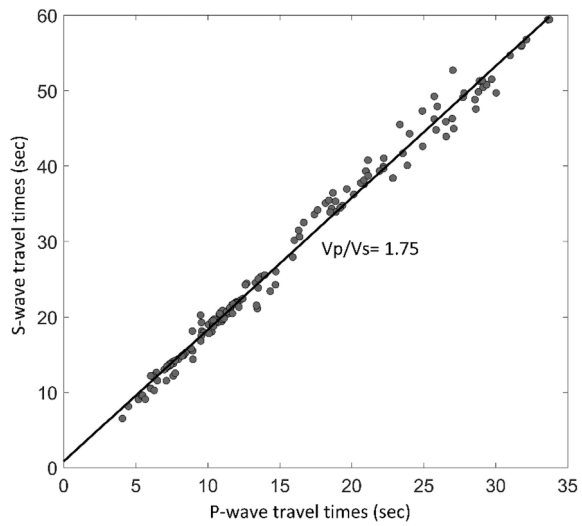

Fig. 5 Wadati diagram for the events used in this study. The estimated Vp/Vs ratio is 1.75

Fig. S6 and Fig. S7, respectively. We identified local earthquakes in four regions: Region 1 located west-southwest (WSW) of Mt. Salak, Region 2 located north of Mt. Gede, Region 3 located south of Purwakarta, and Region 4 located on the Baribis Fault (Fig. 7b). From August to September 2019, there was a swarm of earthquakes in Region 1, which occurred ~ 13 km WSW of Mt. Salak-Bogor, West Java (Fig. 7b). Based on the BMKG report, the magnitude of these events varied from M 2.2 to M 4.2. Several of the events were felt by inhabitants, and one event caused structural damage (M 4.2 on August 23, 2019). Our interpretation of this swarm event is that it was probably related to stress changes due to volcano tectonic activity. Supendi et al. (2018) showed that a destructive earthquake occurred in this area on September 8, 2012 (M_L 4.6) along a thrust fault. In Region 2, we found seven earthquakes located ~ 12 km north of Mt. Gede (Fig. 7b). The three earthquakes that occurred in Region 3 were probably caused by an unidentified local fault in the region.

Finally, in Region 4, we identified two events on the Baribis Fault on December 10, 2019 (Mw 3.0) and March 29, 2020 (Mw 3.2). We note that the December 10 event was felt in Bekasi where it registered II-III MMI (Fig. 7b). We also conducted focal mechanism analysis in order to estimate the type of fault slip for Region 4 events. The two focal mechanism solutions of the events located close to the Baribis Fault (see Additional file 1: Fig. S8 for location uncertainties) reveal a thrust fault dipping southwards (Fig. 7b). While both focal mechanism solutions are consistent with thrust faulting, there are notable differences in strike and dip. These differences are likely due to (1) both earthquakes being of small magnitude, with narrower frequency ranges and lower signal-to-noise ratios, which result in fairly substantial parameter uncertainty; (2) different segments of the Baribis Fault likely having different dip angles. A detailed comparison of the focal mechanism solutions derived from our borehole station data and the BMKG data as well as the combined borehole and BKMG data, along with waveform fitting, is shown in Additional file 1: Figs. S9–S13.

The earthquakes felt in Jakarta and its surroundings are usually located south of West Java, and are related

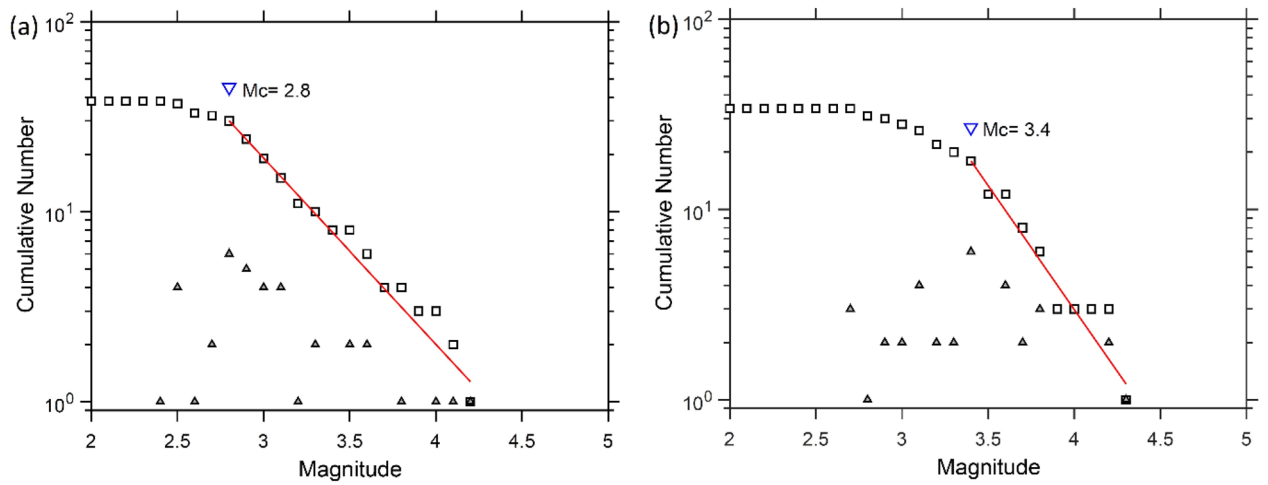

Fig. 6 Earthquake magnitude–frequency relation (Gutenberg–Richter law) for earthquakes that occurred within the blue rectangle shown in Fig. 7a, and were recorded during the same period by **a** borehole stations and **b** BMKG stations. The triangles and squares in the plot depict data and cumulative number of the data, respectively

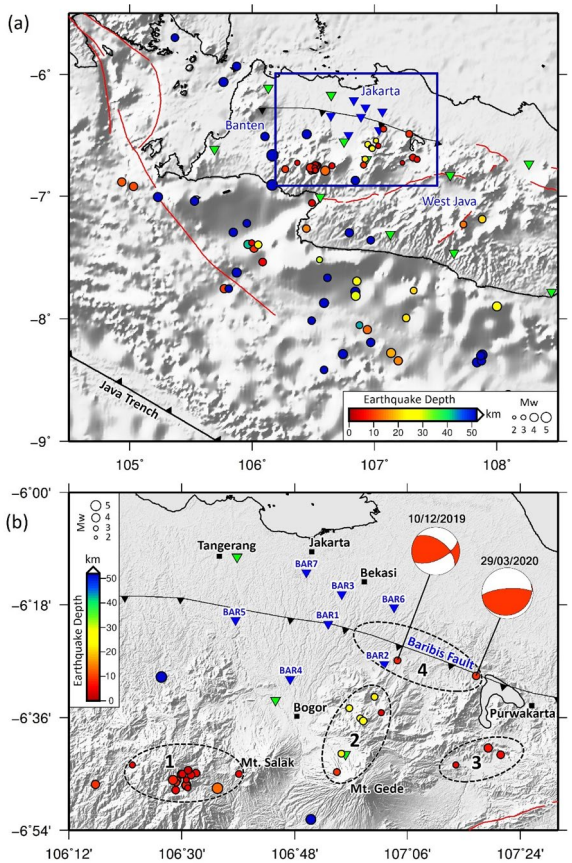

Fig. 7 **a** Map of the earthquakes which were recorded and located using borehole and BMKG seismometers, except Region 2 in which events were not recorded by BMKG stations and located using borehole seismometers only. Blue rectangle shows the location of the study area. **b** Distribution of the inland events divided into four regions. Colored dots depict the focal depth of the hypocenters. Blue and green inverted triangles are the borehole and BMKG seismic stations, respectively, used in this study. The black line represents the Baribis Fault according to Simandjuntak and Barber (1996). Focal mechanism solutions of the December 10, 2019 (Mw 3.0) and March 29, 2020 (Mw 3.2) events with a depth of 8.5 and 9.2 km, respectively, along the Baribis Fault are also shown

to subduction zone processes along the Java Trench. However, the earthquake felt in Bekasi on December 10, 2019, was located inland and close to the Baribis Fault line, indicating that it is probably active. This new seismic evidence is important, and suggests that the Baribis Fault should be considered when updating our national hazard maps since its hazard potential is not considered in the current generation of maps (Irsyam et al. 2017, 2020). This is for the simple reason that its status as an active or inactive fault was not known when the hazard maps were assembled.

Conclusions

We deployed seven borehole seismometers in and around Jakarta to monitor earthquakes in the region. The new data, which are more sensitive to small events compared to the existing surface network run by BMKG, allow us to address fundamental scientific questions about the Baribis Fault near Jakarta, in particular whether it is currently active or not. Our observations and results indicate that an earthquake felt in Bekasi was located very close to the Baribis Fault line (~ 1.8 km south of the fault), and had a focal mechanism consistent with an oblique thrust fault. Another event was also recorded close to the eastern part of the Baribis Fault line with a reverse mechanism. These two events may be evidence that the Baribis Fault is active, which has important implications for seismic hazard in the megacity of Jakarta. In addition, we identified three seismically active regions: Region 1 located west-southwest of Mt. Salak-Bogor, Region 2 located north of Mt. Gede-Bogor, and Region 3 located south of Purwakarta. The seismicity in these regions require further study to understand whether they are related to volcanic or tectonic processes.

Supplementary Information

The online version contains supplementary material available at https://doi.org/10.1186/s40562-021-00209-4.

Additional file 1. Additional figures and tables.

Acknowledgements

The authors are grateful to the BMKG for access to their earthquake data used in this study. This study was supported by the Institut Teknologi Bandung (Riset KK A, ITB, 2019/2020) and PT. Reasuransi Maipark, Jakarta, and also partly by the Indonesian Ministry of Education, Culture, Research and Technology under World Class University (WCU) Program managed by Institut Teknologi Bandung awarded to SW. All figures were made using the Generic Mapping Tools (Wessel and Smith 1998). The authors thank the two reviewers for constructive reviews of the original version of this manuscript.

Authors' contributions

RD conceived the study together with PS and SW; RD, PS, AA, and HAS performed the data processing, and analyzed the results together with SW, EG, DPS, and NR; RD, PS, SW, NR, and EG wrote the manuscript. ZZ and RD led the field work supported by YMH, DPS, and PS. All the authors have reviewed and contributed to the preparation. All the authors read and approved the final manuscript.

Funding

This study was supported by the Institut Teknologi Bandung (Riset KK A, ITB, 2019/2020) and PT. Reasuransi Maipark, Jakarta.

Availability of data and materials

Earthquake catalog data are available in the supplementary material (Additional file 1: Table S1), and waveform data will eventually be made available (once the study is completed) at https://www.maipark.com/index.php/en/rdi/maipark_research_data.

Declarations

Competing interests

The authors declare that we have no significant competing financial, professional, or personal interests that might have influenced the performance or presentation of the work described in this manuscript.

Author details

[1]Geophysical Engineering Study Program, Faculty of Mining and Petroleum Engineering, Institut Teknologi Bandung, Bandung 40132, Indonesia. [2]PT. Reasuransi Maipark, Multivision Tower, Menteng Atas, Jakarta 12960, Indonesia. [3]Agency for Meteorology, Climatology, and Geophysics (BMKG), Jakarta 10720, Indonesia. [4]Department of Earth Sciences-Bullard Labs, University of Cambridge, Cambridge CB30EZ, UK. [5]Global Geophysics Research Group, Faculty of Mining and Petroleum Engineering, Institut Teknologi Bandung, Bandung 40132, Indonesia. [6]Faculty of Engineering, Maranatha Christian University, Bandung 40164, Indonesia. [7]Department of Earth Science, University of Bergen, Allègaten 41, 5007 Bergen, Norway.

Received: 24 May 2021 Accepted: 19 December 2021
Published online: 31 December 2021

References

Botev Z, Grotowski J (2010) Kernel density estimation via diffusion. Ann Stat 38(5):2916–2957. https://doi.org/10.1214/10-AOS799

Botev Z (2016) Adaptive kernel density estimation in one-dimension. MATLAB Central File Exchange, retrieved on April 20, 2020

Bouchon M (1981) A simple method to calculate Green's functions for elastic layered media. Bull Seismol Soc Am 71(4):959–971

Cipta A, Cummins P, Dettmer J, Saygin E, Irsyam M, Rudyanto A, Murjaya J (2018) Seismic velocity structure of the Jakarta Basin, Indonesia, using trans-dimensional Bayesian inversion of horizontal-to-vertical spectral ratios. Geophys J Int 215:431–449. https://doi.org/10.1093/gji/ggy289

Daryono M, Natawidjaja DH, Sapiie B, Cummins P (2018) Earthquake geology of the Lembang Fault, West Java Indonesia. Tectonophysics 751:2

Gunawan E, Widiyantoro S (2019) Active tectonic deformation in Java, Indonesia inferred from a GPS-derived strain rate. J Geodyn 123:49–54. https://doi.org/10.1016/j.jog.2019.01.004

Havskov J, Ottemöller L (2010) Introduction. in Routine Data Processing in Earthquake Seismology, pp. 1–14, Dordrecht: Springer Netherlands. https://doi.org/10.1007/978-90-481-8697-6_1

Irsyam M, Cummins PR, Asrurifak M, Faizal L, Natawidjaja DH, Widiyantoro S, Meilano I, Triyoso W, Rudiyanto A, Hidayati S, Ridwan M, NR, and SyahbanaAJ, (2020) Development of the 2017 national seismic hazard maps of Indonesia. Earthq Spectra 36:1–25. https://doi.org/10.1177/8755293020951206

Irsyam M, Widiyantoro S, Natawidjaya DH, Meilano I, Rudyanto A, Hidayati S, Triyoso W, Hanifa NR, Djarwadi D, Faizal L, Sunarjito (2017) Map of sources and hazards of the 2017 Indonesian earthquake, Center for Research and Development of Housing and Settlements, Ministry of Public Works and Housing, the Republic of Indonesia (in Indonesian)

Katili JA, Soetadi R (1971) Neotectonics and seismic zones of the Indonesian Archipelago. New Zealand Royal Soc Bull 9:39–45

Kennett BLN, Engdahl ER, Buland R (1995) Constraints on seismic velocities in the earth from traveltimes. Geophys J Int 122:108–124. https://doi.org/10.1111/j.1365-246X.1995.tb03540.x

Koulakov I, Bohm M, Asch G, Lühr BG, Manzanares A, Brotopuspito KS, Fauzi PMA, Puspito NT, Ratdomopurbo A, Kopp H, Rabbel W, Shevkunova E (2007) P and S velocity structure of the crust and the upper mantle beneath central Java from local tomography inversion. J Geophys Res 112:B08310. https://doi.org/10.1029/2006JB004712

Koulali A, McClusky S, Susilo S, Leonard Y, Cummins P, Tregoning P, Meilano I, Efendi J, Wijanarto AB (2017) The kinematics of crustal deformation in Java from GPS observations: Implications for fault slip partitioning. Earth Planet Sci Lett 458:69–79. https://doi.org/10.1016/j.epsl.2016.10.039

Lahr JC (1979) Open-File Report (Open-File Rep No 79–431). USGS Publications Warehouse. https://doi.org/10.3133/ofr79431

Lahr JC (1989) HYPOELLIPSE: A computer program for determining local earthquake ypocentral parameters, magnitude and first motion pattern (Y2K compliant version), US Geol Surv Open-File Rep., 92 pp

Lomax A, Michelini A (2009) Mwpd: a duration–amplitude procedure for rapid determination of earthquake magnitude and tsunamigenic potential from P waveforms. Geophys J Int 176:200–214. https://doi.org/10.1111/j.1365-246X.2008.03974.x

Lomax A, Satriano C, Vassallo M (2012) Automatic picker developments and optimization: filterpicker–a robust, broadband picker for real-time seismic monitoring and earthquake early warning. Seismol Res Lett 83:531–540. https://doi.org/10.1785/gssrl.83.3.531

Miller MS, O'Driscoll LJ, Roosmawati N, Harris CW, Porritt RW, Widiyantoro S, Teofilo da Costa L et al (2016) Banda arc experiment—transitions in the banda arc-australian continental collision. Seismol Res Lett 87:1417–1423. https://doi.org/10.1785/0220160124

Musson RMW (2012) A provisional catalogue of historical earthquakes in Indonesia. British Geol Surv Open Rep OR/12/073, Edinburgh, 21 pp.

Nguyen N, Griffin J, Cipta A, Cummins P (2015) Indonesia's historical earthquakes: Modelled examples for improving the national hazard map. https://doi.org/10.11636/Record.2015.023

Peterson J (1993) Observations and modeling of seismic background noise. US Geol Surv Open-File Rep. https://doi.org/10.3133/ofr93322

Ridwan M, Widiyantoro S, Irsyam M, Afnimar YH (2016) Development of an engineering bedrock map beneath Jakarta based on microtremor array measurements. Geol Soc London Spec Pub 441:153–165. https://doi.org/10.1144/SP441.7

Ridwan M, Cummins PR, Widiyantoro S, Irsyam M (2019) Site characterization using microtremor array and seismic hazard assessment for Jakarta Indonesia. Bull Seismol Soc Am 109(6):2644–2657. https://doi.org/10.1785/0120190040

Rosalia S, Cummins P, Widiyantoro S, Yudistira T, Nugraha AD, Hawkins R (2019) Group velocity maps using subspace and transdimensional inversions: ambient noise tomography in the western part of Java Indonesia. Geophys J Int 220(2):1260–1274. https://doi.org/10.1093/gji/ggz498

Saygin E, Cummins PR, Cipta A, Hawkins R, Pandhu R, Murjaya J, Masturyono IM, Widiyantoro S, Kennett BLN (2016) Imaging architecture of the Jakarta Basin, Indonesia with transdimensional inversion of seismic noise. Geophys J Int 204(2):918–931. https://doi.org/10.1093/gji/ggv466

Saygin E, Cummins PR, Lumley D (2017) Retrieval of the P wave reflectivity response from autocorrelation of seismic noise: Jakarta Basin, Indonesia. Geophys Res Lett 44:792–799. https://doi.org/10.1002/2016GL071363

Setyadji B, Murata I, Kahar J, Suparka S, Tanaka T (1997) Analysis of GPS measurement in West-Java, Indonesia. Ann Disas Prev Res Inst Kyoto Univ. 40, B-1: 27–33. http://hdl.handle.net/2433/80196

Simandjuntak TO, Barber AJ (1996) Contrasting tectonic styles in the Neogene orogenic belts of Indonesia. Geol Soc London Spec Pub 106:185–201. https://doi.org/10.1144/GSL.SP.1996.106.01.12

Sokos EN, Zahradnik J (2008) ISOLA a Fortran code and a Matlab GUI to perform multiple-point source inversion of seismic data. Comput Geosci 34:967–977. https://doi.org/10.1016/j.cageo.2007.07.005

Stein S, Wysession M (2003) An introduction to seismology, earthquakes, and earth structure, Malden, MA: Blackwell Pub. ISBN: 978–0–865–42078–6

Supendi P, Nugraha AD, Puspito NT, Widiyantoro S, Daryono WSH (2018) Identification of active faults in West Java, Indonesia, based on earthquake hypocenter determination, relocation, and focal mechanism analysis. Geosci Lett. https://doi.org/10.1186/s40562-018-0130-y

Wessel P, Smith WHF (1998) New, improved version of generic mapping tools released. Eos Trans Am Geophys Union 79:579. https://doi.org/10.1029/98EO00426

Wichmann A (1918) Die Erdbeben des Indischen Archipels bis zum Jahre 1857. Verh. der K. Akad. van Wet. Te Amsterdam 20(4): 193 **(in German)**

Publisher's Note

Springer Nature remains neutral with regard to jurisdictional claims in published maps and institutional affiliations.